



Linkages between land cover change, lake shrinkage, and sublacustrine influence determined from remote sensing of select Rift Valley Lakes in Kenya

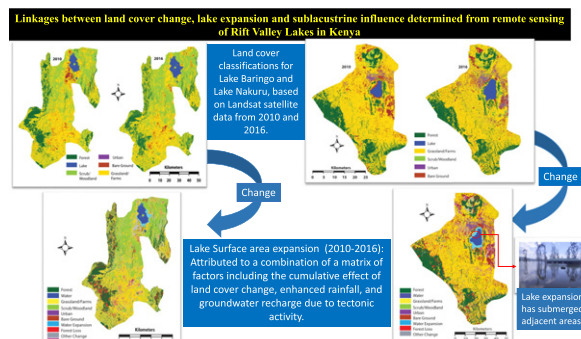
Lawrence M. Kiage ^{*}, Paul Douglas

Department of Geosciences, Georgia State University, Atlanta, GA 30303, USA

HIGHLIGHTS

- Surface area change in four Rift Valley lakes was derived from MNDWI for 1984–2018.
- NDVI used to estimate lake surface area covered by algae for 1984–2018.
- Land cover change provides information on primary causes of change in surface area.
- Remarkable change in surface area after 2010 linked to multiple causations.

GRAPHICAL ABSTRACT



ARTICLE INFO

Article history:

Received 11 November 2019

Received in revised form 6 December 2019

Accepted 7 December 2019

Available online 9 December 2019

Editor: José Virgílio Cruz

Keywords:

Land use and land cover change

Rift Valley lakes

MNDWI

NDVI

Landsat data

Lake surface area dynamics

ABSTRACT

The Great Rift Valley system is home to many volcanic and tectonic lakes including some of the world's oldest and deepest lakes. These lakes host a rich heritage of biodiversity that is endangered by recent drastic hydrologic changes due to multiple natural and anthropogenic stressors in the catchment areas of some of the lakes. This study utilized Landsat TM, ETM+, and OLI data to conduct a systematic investigation of the relationship between hydrological dynamics in the basins of four Rift Valley lakes (Nakuru, Baringo, Bogoria, and Elementaita) and recent land cover and land-use change. The Modified Normalized Difference Water Index (MNDWI) proved to be more accurate and robust for delineating water surface areas when compared to the output of Normalized Difference Vegetation Index (NDVI) and classification algorithms. NDVI was successful when delineating water surface at Lake Baringo but not in Lakes Bogoria, Nakuru, and Elementaita, whose surfaces were dominated by algae. All the lakes expanded substantially after 2010 submerging surrounding areas leading to disruption of livelihoods, property damage, and displacement of thousands of people. The recent drastic hydrologic changes have multiple causations including land cover and land use change, increase in rainfall, and possible change in geogenic water input due to tectonic activity. The rapid rise in water levels appears to have altered the biogeochemical balance of the hypersaline lakes with severe ramifications on the rich biodiversity that is supported by the lakes.

© 2019 Elsevier B.V. All rights reserved.

* Corresponding author.

E-mail address: lkiage@gsu.edu (L.M. Kiage).

1. Introduction

The Great Rift Valley system, also known as the Gregory Rift Valley system, runs on a north-south axis through the eastern side of the African continent. The Rift Valley, which is a product of separation of the Nubian and the Somali plates in Africa, is home to over 30 volcanic and tectonic lakes including some of the world's oldest and deepest lakes (Fazi et al., 2018). These lakes and their environments host a rich heritage of biodiversity, some of which is now considered endangered due to environmental and climatic changes in the East African tropics (Krienitz et al., 2016). The danger to biodiversity is linked to recent drastic hydrologic changes in the region attributed to a combination of multiple natural and anthropogenic stressors in the catchment areas of the lakes. The hydrological dynamics are most pronounced in endorheic basins and those lacking surface outflow such Lakes Baringo, Bogoria, Nakuru and Elementaita in Kenya. Since 2010 these four lakes have experienced a remarkable rise in their waters that has submerged surrounding areas, disrupted livelihoods, damaged property, and displaced thousands of people.

Some hypotheses have been proposed to explain the hydrological changes in the Rift Valley lakes including deforestation and increased runoff in the drainage basins, unpredictable precipitation patterns due to shifting location of the Intertropical Convergence Zone (ITCZ), El Niño Southern Oscillation (ENSO) events, and tectonic activity, among others. Satellite remote sensing technologies present a significant opportunity in efforts aimed at understanding whether there are spatio-temporal changes in land cover and land use in the drainage basins of the lakes that may explain the hydrologic dynamics. Imagery acquired by instruments aboard the Landsat series of satellites have proven useful for monitoring recent environmental changes in land cover including differences in water surface area (Alamgir et al., 2016; Halabisky et al., 2016; Wang et al., 2018; Wang and Feng, 2011; Zhang et al., 2019). Considering their long history of archiving continuous, consistent, and systematic coverage of large areas at fine temporal and spatial scales, the Landsat series provides excellent data sources for investigating basinwide environmental dynamics involving visible water extent and changes in land cover in the watersheds of the Rift Valley lakes.

Satellite remote sensing technologies offer the scientific community powerful tools for estimating changes in water quality and quantity that can be both cost-effective and sustainable (Gao et al., 2010; Scharsich et al., 2017; Toure et al., 2018). Access to and use of remote sensing data such as those of the Landsat series of satellites provide part of the solution to the high costs and logistical quagmires of traditional in situ watershed assessments that are typically associated with monitoring large drainage basins and lakes. Not only do satellite data provide spatiotemporal coverages, they also enable simultaneous monitoring of multiple lakes at reduced costs. Satellite data on land cover and land use change in the lakes' watersheds can be amalgamated with meteorological data to provide information that aids our understanding of the driving mechanisms of the hydrological changes in the Rift Valley lakes. This study utilized Landsat data to conduct a systematic investigation of the relationship between hydrological dynamics in the four Rift Valley lakes (Nakuru, Baringo, Bogoria, and Elementaita) and cumulative land cover and land-use change.

1.1. Study area

The four lakes that constitute the study area are located within the eastern branch of the Rift Valley in western Kenya (Fig. 1). Although there is a significant difference in vegetation due to elevation on a north-south axis, the area is primarily characterized by a sub-humid to a semi-arid climate that supports savanna vegetation complex characterized by open Acacia scrubland but with denser tree cover at higher elevations, and along streams. Rainfall is low in the rift floor where it annually averages about 700 mm but is much higher in the adjacent highlands (>2500 mm) (Kiage et al., 2007). The rains come in two seasons

that are primarily controlled by the ITCZ. Capricious downpours characterize the rains which fall within a few weeks in the months of March–May and October–December, that define the long and short rain seasons, respectively. There are variations in the rainfall pattern and totals on a range of timescales determined by ENSO episodes, i.e., every 5–7 years (LaVigne and Ashley, 2002). Temperatures in the region range from 14 °C to 35 °C with typical diurnal maxima and minima of 28 °C–35 °C and 14 °C–18 °C, respectively.

Lake Baringo, which extends from approximately 0° 40' N to 0° 43' N, and 35° 18' E to 36° 20' E, is the farthest north and lies at an altitude of 970 m above sea level with a catchment of 6200 km². The lake occupies the southern end of a half-graben depression in the central Kenya Rift Valley and is unique in the sense that it is one of the two lakes (Lake Naivasha is the other) in the Gregory Rift that has fresh water even though it has no surface outlet. It is hypothesized that Lake Baringo owes its fresh water to seepage through sediments into underlying faulted volcanic bedrock. The lake is renowned for its large populations of hippopotamus, crocodiles, and the over 500 avifaunal species it supports.

Lake Bogoria which extends from 0° 10' N to 0° 20' N and 36° 04' E to 36° 26' E, at an elevation of 992 m above sea level, is located some 20 km due south of Lake Baringo. The two lake basins are separated by the Lobi Plain which constitutes a drainage divide that rises to about 1000 m above sea level. Lake Bogoria occupies the same half-graben depression that hosts Lake Baringo but is served by a much smaller drainage basin of about 705 km². The endorheic basin of Lake Bogoria influences its salinity (total dissolved solids of 60–100 g l⁻¹) and alkalinity (pH: 10.3–10.5), a product of sodium, carbonate, hydrocarbon and chloride ions (Renaut et al., 2017). The hypersalinity of the lake is exacerbated by inflow from saline hot springs that straddle the western shore of its basin and high evaporation rates that far exceed precipitation. Lake Bogoria is a designated National Reserve which, like the nearby Lake Baringo, also supports a rich biodiversity that includes a large number of bird species, buffalo, baboon, caracal, cheetah, spotted hyena, warthog, impala, and zebra, among others.

Lake Nakuru is located 53 km from the southern edge of Lake Bogoria at an elevation of 1754 m above sea level. Like most of the lakes in the Rift Valley, it has an endorheic basin characterized by hypersalinity with conductivity values of up to 160,000 µS/cm. The lake has a maximum depth of 1.8 m and presently extends from 0° 18' S to 0° 24' S and 36° 03' E to 36° 07' E. It is part of Lake Nakuru National Park, a protected area under the Ramsar Convention on wetlands, which is (was) best known for its millions of pink flamingos (both lesser and greater) that used to nest on its shores. The lake's environment hosts many other avifaunal species as well as hosts of buffalos, warthogs, baboons, gazelles, lions, leopards, and other large mammals. In addition to precipitation, Lake Nakuru is fed by effluent of the nearby Nakuru City sewerage treatment system, and three seasonal surface streams (Raini, 2009).

Lake Elementaita is located just 12 km to the southeast of Lake Nakuru, at an elevation of 1786 m above sea level. It is highly alkaline (sodium carbonate salts) and presently shallow (<1 m) with hypersaline waters (conductivity between 12,000 and 40,000 µS/cm) that extend from 0° 24' S to 0° 28' S, and 36° 12' E to 36° 16' E. The lake is thought to be a shrunken remnant of a much larger paleolake that occupied the Nakuru–Elementaita basin which has a drainage area of 2390 km² (Murimi, 1993; Dühnforth et al., 2006). Its basin is bounded by the Mau Escarpment to the west, Bahati–Kinangop Plateau to the east and Eburru volcano on the south which forms a divide that separates it from Lake Naivasha basin.

2. Data and methods

Data that were used for this study fall into three categories based on the Landsat satellites that were involved in their acquisition and sensor attributes. The first category consists of Landsat 4 and Landsat 5

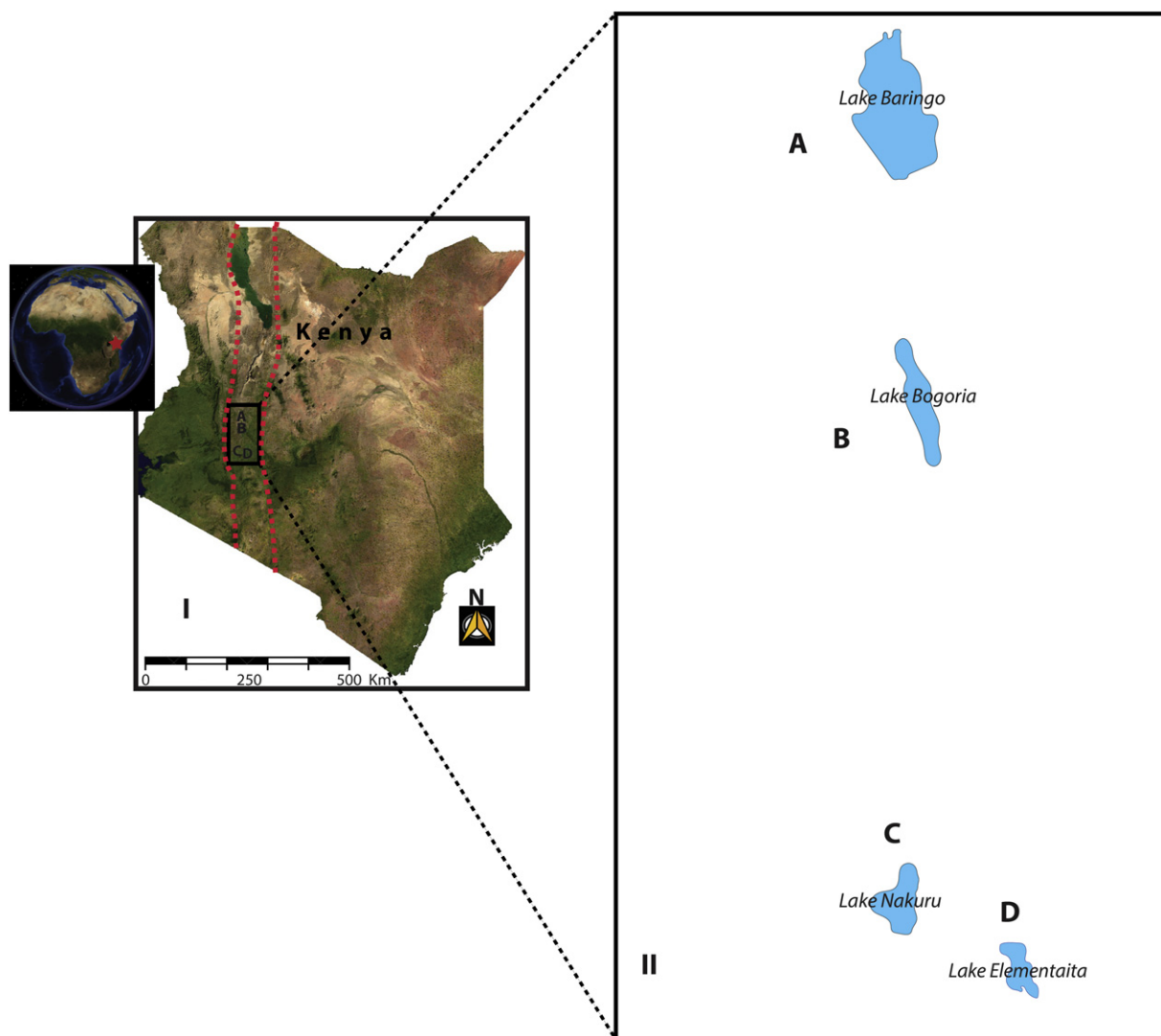


Fig. 1. Location of the study area (marked by a black rectangle) on a satellite image map of Kenya (I). The Rift Valley that runs on a north-south axis is indicated by the dashed red lines. The north-south situation of the lakes that constitute the study area is indicated by the letters A, B, C, and D within the rectangle in I are shown in greater detail in II. Inset is the globe with the study area indicated by a red star on the satellite map of Africa.

satellites which are second generation Landsat satellites that carry the Thematic Mapper (TM) sensor on a Multimission Modular Spacecraft. Landsat 4/5 platforms were designed by NASA to improve the

acquisition and transmission of data by utilizing a more sophisticated sensor, and to offer rapid data processing at an automated processing facility. TM data offer better geometric performance as well as spectral,

Table 1
Attributes of the Landsat data used in the study.

Acquisition date	Path/row	Sensor	Spatial resolution (m) ^a	No. of bands ^b	Sun elevation	Sun azimuth
July 1, 1984	169/60	TM5	30	7	48.28	53.89
January 28, 1986	169/60	TM5	30	7	48.12	117.98
March 1, 1989	169/60	TM4	30	7	52.51	102.49
February 6, 1995	169/60	TM5	30	7	45.21	112.63
January 27, 2000	169/60	ETM+	30	8	53.58	122.4
April 4, 2001	169/60	ETM+	30	8	59.34	79.41
February 2002	169/60	ETM+	30	8	53.15	119.39
February 4, 2003	169/60	ETM+	30	8	53.34	118.07
June 1, 2008	169/60	TM5	30	7	53.84	50.35
June 4, 2009	169/60	TM5	30	7	53.57	49.97
January 30, 2010	169/60	TM5	30	7	53.46	120.63
January 25, 2014	169/60	OLI	30	9	55.24	124.73
February 13, 2015	169/60	OLI	30	9	56.95	115.20
February 16, 2016	169/60	OLI	30	9	57.33	113.62
May 25, 2017	169/60	OLI	30	9	56.86	49.05
February 5, 2018	169/60	OLI	30	9	56.03	119.38

^a Panchromatic band used.

^b Thermal bands were excluded.

radiometric and spatial resolutions when compared to those of the Multispectral Scanner (MSS) sensor that was the mainstay of the first generation of Landsat satellites. The TM sensor has six reflective bands and one thermal band that have a spatial resolution of 30 m and 120 m, respectively. The second category is data from the Landsat 7 satellite that carries the Enhanced Thematic Mapper Plus (ETM+) sensor. The ETM+ sensor has six reflective bands with a spatial resolution of 30 m, a thermal band with 60 m, and includes a 15 m panchromatic band. The third group consists of data acquired by Landsat 8 satellite that operates a two-sensor payload, i.e., the Operational Land Imager (OLI) and the Thermal Infrared Sensor (TIRS). OLI offers eight reflective bands at 30 m spatial resolution and a panchromatic band that has a spatial resolution of 15 m. The OLI bands were designed to provide the same spatial and spectral resolution as those of TM and ETM+ to maintain data continuity. However, OLI has two additional bands, one in the blue (band 1) and the second, an infrared (band 9) for investigations of water resources in coastal areas and detecting cirrus clouds, respectively.

Table 1 is a summary of the georeferenced Level 1 Terrain-Corrected (L1T, cloud cover <10%) Landsat TM/ETM+/OLI data that were assembled for land cover and land use change analyses in the four lakes. Landsat image scenes cover a period of 34 years between 1984 and 2018. The data were accessed and downloaded from the United States Geological Survey (USGS) at <https://earthexplorer.usgs.gov>. The USGS is the repository of Landsat data covering the entire globe. All the image scenes that were selected for analysis had to meet two criteria, that is, near anniversary dates and cloud free over the study area. However, acquiring anniversary dates images, let alone cloud-free ones, from tropical environments is a difficult task because the region has many overcast days throughout the year. Whenever near anniversary scenes could not be found the closest cloud-free coverage was selected. There were no images that met the criteria between 2010 and 2014 in the Landsat archive which, unfortunately, coincides with a critical period of change in land cover. Rainfall data for study area, which were key to interpreting the land cover changes, were acquired from the Kenya Meteorological Department in Nairobi.

2.1. Image preprocessing

Some image preprocessing procedures were performed on the Landsat data to clean up any inherent errors before performing detailed analyses. Preprocessing included radiometric and atmospheric correction, geometric correction, and image subset. Radiometric correction is performed to calibrate pixel values in the image by removing the influence of the atmosphere due to the sun's azimuth and elevation, sensor viewing geometry, terrain characteristics, and atmospheric conditions at the time of acquisition. This procedure is necessary whenever a comparison involving multiple datasets is involved. In this study, the radiometric and atmospheric correction was performed by converting raw digital numbers (DN) in Landsat into top-of-atmosphere radiance or at-sensor radiance values using ATCOR algorithm in ERDAS imagine 2018. The ATCOR algorithm is a large database that contains the results of radiative transfer calculations based on the Modtran R 5 code ([Berk et al., 1998](#)). Calibration of raw DN to radiance is expressed in the following equation:

$$L\lambda = c_0 + c_1 * DN \quad (1)$$

where $L\lambda$ is the at-sensor radiance value while c_1 and c_0 are radiometric calibration coefficients consistent with the sensor's gain and offset, respectively.

The Landsat images were georeferenced to topographical maps of 1:50000 covering the Lakes Nakuru and Baringo areas into UTM-WGS1984 coordinate system and backed up by ground control points (GCPs) from Digital Globe images displayed in Google Earth with an accuracy of <5 m. Georeferencing or geometric correction is an image

preprocessing procedure that is necessary whenever multi-temporal image analysis is performed, especially where land cover change is assessed using satellite imagery ([Zhang and Roy, 2016](#)). The geometric correction was performed using the multipoint geometric correction tool, and polynomial transformation in ERDAS imagine 2018. The geometric correction involved selecting 50 ground control points (GCPs) and Root Mean Square (RMS) error of <0.5 of a pixel. The GCPs that were chosen were not only clearly visible on the maps, Google Earth, and the reference Landsat image, but had to be evenly distributed throughout the images. They included road junctions, and permanent buildings including schools, churches, and government buildings.

The last preprocessing procedure that was performed is image subsetting. This procedure was necessary considering that Landsat image scenes cover large areas of about 185 km². Subsetting made it possible to retrieve only the areas of interest (watersheds) from Landsat scenes.

2.2. Image classification and spectral enhancement

The primary purpose of performing spectral enhancement and data transformation is to highlight changes in surface reflectance. This facilitates the delineation of the lake surface area and the spatial cover of features on the area represented in the images. Three main techniques were utilized in this study, including the use of spectral indices and post-classification image differencing. Before the techniques were applied, the lake areas were subset into the area of interest in ERDAS imagine 2018. Two spectral indices, i.e., Modified Normalized Difference Water Index (MNDWI) and Normalized Difference Vegetation Index (NDVI) were adopted for this study and used to delineate the lake surface. The choice of the index to use for mapping water has a significant influence on the accuracy achieved. Multiple studies from different parts of the world (e.g. [Acharya et al., 2018](#); [Buma et al., 2018](#); [Mohammadi et al., 2017](#); [Liang and Yan, 2017](#); [Yang et al., 2018](#); [Wang et al., 2018](#)) have demonstrated the effectiveness if using the MNDWI to extract data that delineates water bodies from other features on the Earth surface. The MNDWI has the capability of straining plants and impervious surface areas thereby revealing subtle water features while eliminating shadow effects. In Landsat MNDWI is computed as follows:

$$MNDWI = (\text{Green} - \text{SWIR1}) / (\text{Green} + \text{SWIR1}) \quad (2)$$

where Green is the reflectance radiated in the green waveband (520–600 nm), and SWIR1 is the reflectance emitted in the shortwave infrared waveband (1550–1750 nm) of the satellite radiometer. The MNDWI yields values fluctuating between −1 and +1. Water surfaces generate positive values due to higher absorption in the mid-infrared (shortwave infrared) while other surfaces such as cultural features, soils, and vegetation produce negative values ([Xu, 2006](#)).

Table 2
Land cover classes used in the study.

Land cover	Code	Description
Water	1	Mostly water in lakes, on rivers, artificial reservoirs, and sewerage treatment plants.
Bare ground	2	Areas with exposed soils or rock including cultivated farmland.
Grassland and farmland	3	Environments dominated by grass including savanna vegetation, and/or pastureland. Farmlands are distinguished by linear and rectangular-shaped features.
Scrubland/woodland	4	Areas dominated by shrubs with many stems and other woody plants that are <8 m and some open areas covered by grass.
Urban	5	Areas dominated by buildings in close proximity and road networks.
Forest	6	Environments characterized by dense tree cover.

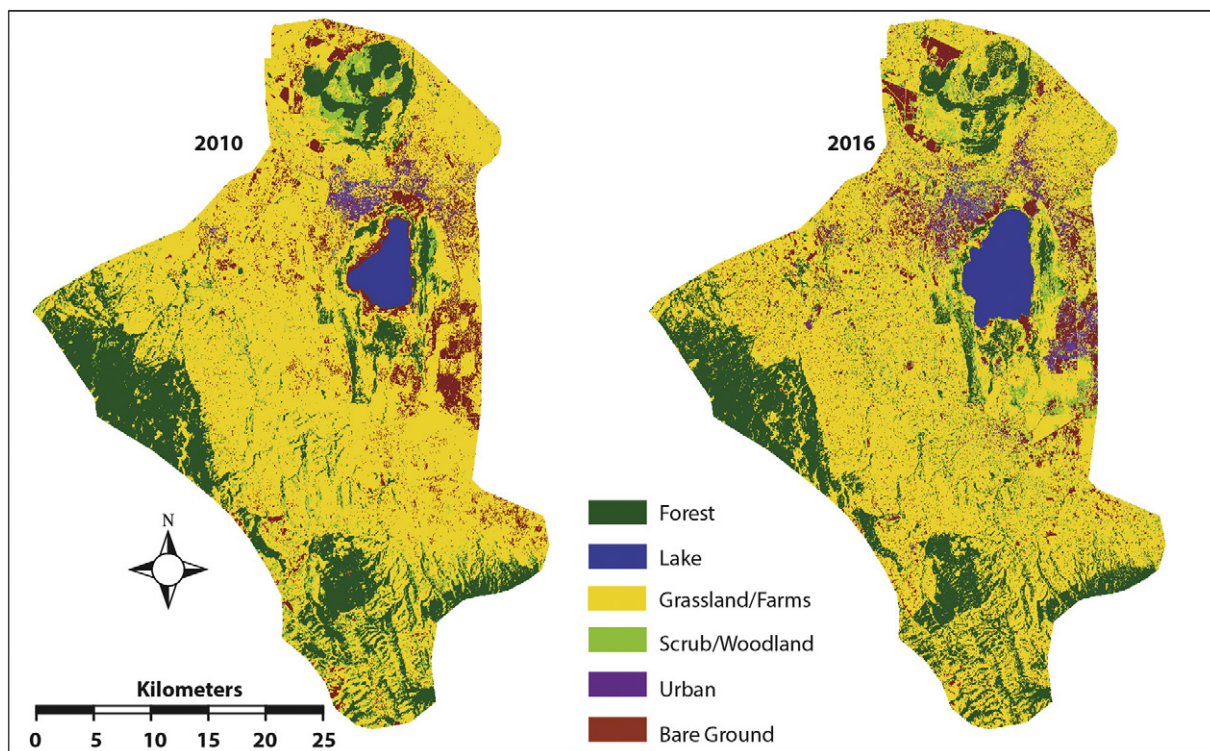


Fig. 2. Land-cover maps for Lake Nakuru drainage basin derived from unsupervised classification of the 2010 TM and 2016 OLI images.

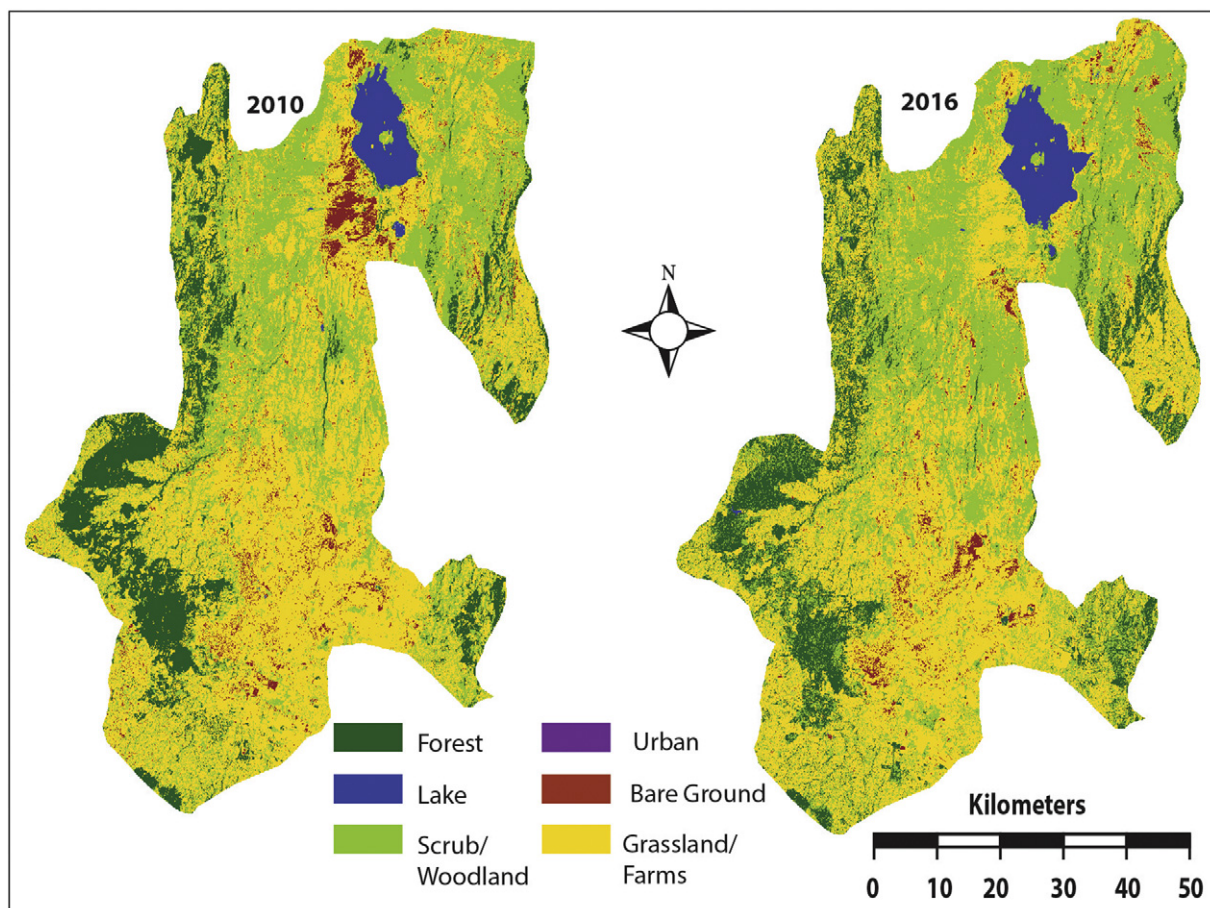


Fig. 3. Land-cover maps for Lake Baringo drainage basin derived from unsupervised classification of the 2010 TM and 2016 OLI images.

NDVI is perhaps the most commonly used index for remote sensing of vegetation but can also delineate water surfaces when an appropriate threshold is applied (Jiang et al., 2012, 2014; Kiage and Walker, 2009; Kiage and Obuoyo, 2011; Rokni et al., 2014). The index is computed as follows:

$$\text{NDVI} = (\text{NIR} - \text{RED}) / (\text{NIR} + \text{RED}) \quad (3)$$

where NIR is the reflectance from the near-infrared band (760–900 nm), and RED is the reflectance radiated in the visible red band (630–690 nm). NDVI values range from -1 to $+1$, with negative values being associated with water surfaces while positive values correspond with vegetation. In this study NDVI was performed on satellite data to assess land cover change through time, estimate algae cover on the lakes, and as a check on the effectiveness of the MNDWI.

Image classification was performed on each image to provide a platform for assessing land cover change in the study area and to relate the changes in the watersheds to the changes in the surface area of the lakes. The spectral classes were grouped into six informational land cover classes including water (mostly lake), bare ground, grassland/farms, scrubland/woodland, urban/cultural and forest (Table 2). These land cover classes varied from one drainage basin to the another depending on climate and level of urbanization. The classified images were subjected to accuracy assessment following the methods described by Congalton and Green (1999). Accuracy assessment was performed in ERDAS imagine by comparing land cover classes assigned to 200 randomly generated GPS points spread throughout the watersheds

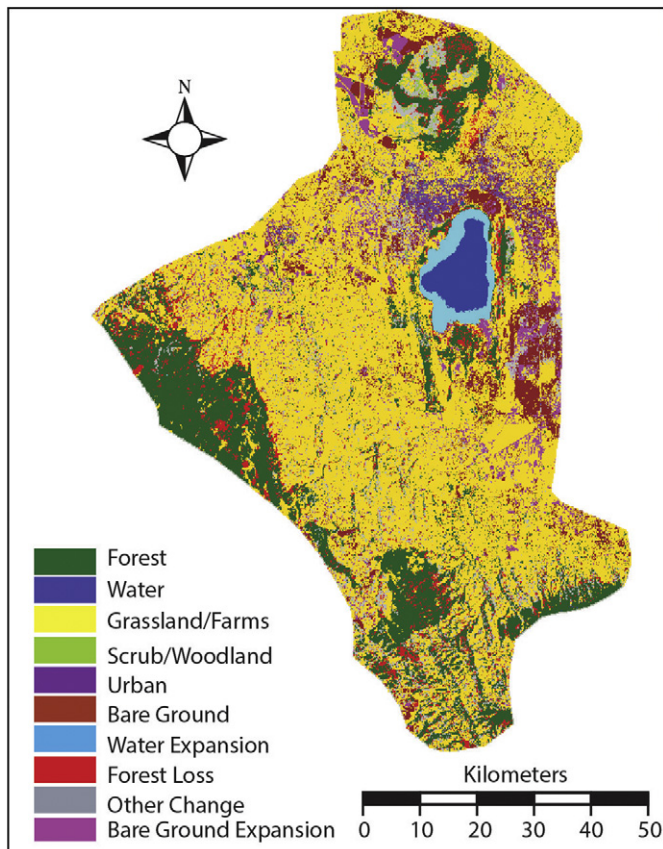


Fig. 4. Change-detection map for Lake Nakuru drainage basin derived from a comparison of the 2010 and 2016 land cover classification maps. The most outstanding change involves the lake surface (whose expansion is represented by cyan color), urban class (purple), forest (loss represented in red color) and the bare surface class (represented magenta color). (For interpretation of the references to color in this figure legend, the reader is referred to the web version of this article.)

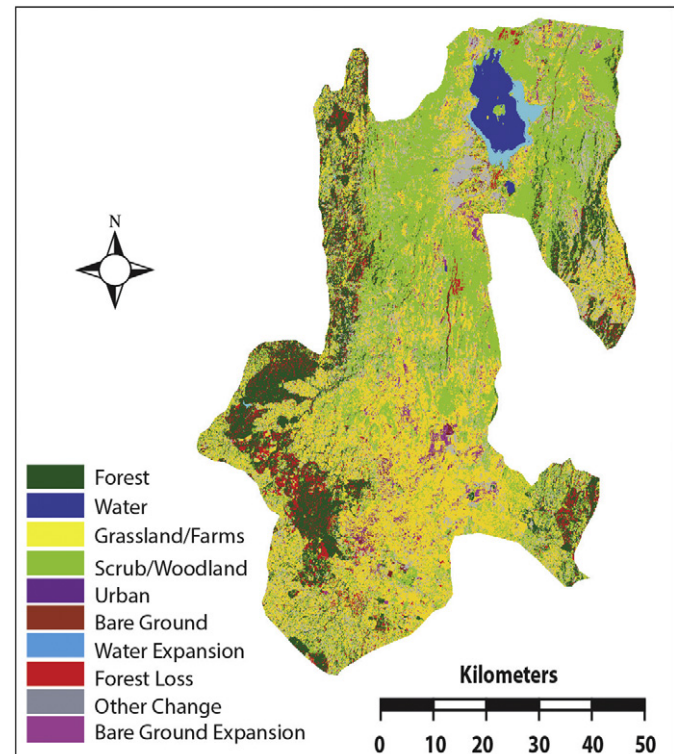


Fig. 5. Change-detection map for Lake Baringo drainage basin derived from a comparison of the 2010 and 2016 land cover classification maps. The most outstanding change involves the lake surface (whose expansion is represented by cyan color), urban class (purple), forest (loss represented in red color) and the bare surface class (represented magenta color). (For interpretation of the references to color in this figure legend, the reader is referred to the web version of this article.)

with corresponding points on high-resolution Google Earth images for the specific years.

3. Results

This study focused on detailed analysis of change in land cover on Lakes Baringo and Nakuru—the two lakes that experienced the most expansion in surface area over the four years between 2010 and 2016. The study generated maps representing the status of land cover and change between 2010 and 2016 (Figs. 2 and 3). Unsupervised classification yielded maps with high overall classification accuracies ranging between 91.4% and 98.1% with overall Kappa Statistics between 0.88 and

Table 3

Lake surface area (in km²) computed using the MNDWI and verified using supervised classification.

Year	Baringo (NDVI)	Bogoria	Elementaita	Nakuru
1984	149	145	32.8	18.6
1986	144	141	32.1	17.7
1989	134	131	32.9	19.3
1995	120.1	118.5	32.6	16.6
2000	131.2	126	30.1	20.5
2001	123.6	120.2	33.6	15.5
2002	120.6	117.2	33.9	19.3
2003	111.8	108.5	33.5	18.8
2008	138.2	135.7	33.9	18.8
2009	138.2	135.2	33.5	16.5
2010	136.1	133.2	33.4	15.9
2014	193.3	189.4	38.9	22.1
2015	192.7	189.4	38.7	21.5
2016	194.1	186.4	39	21.6
2017	183.5	177.4	38.1	20.7
2018	183.4	180.9	35.9	20.5
				54.3

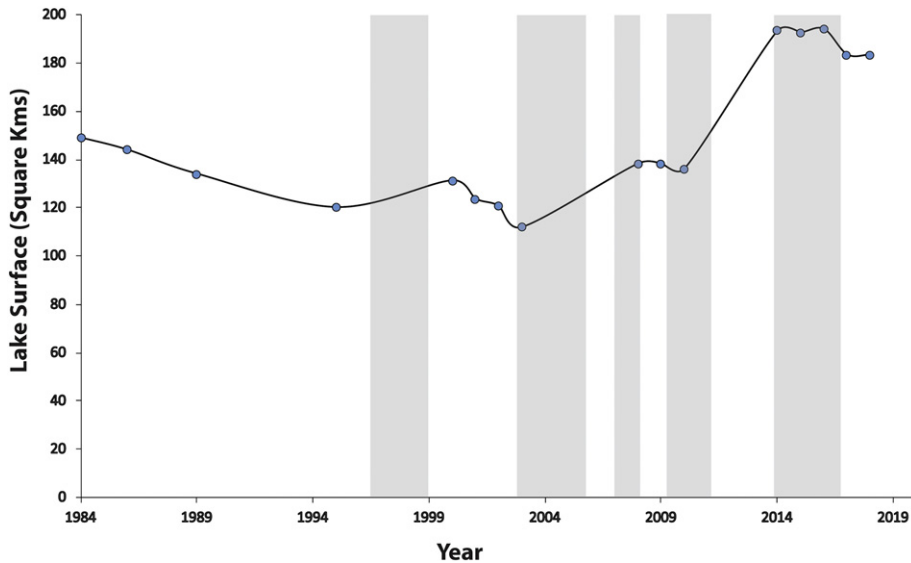


Fig. 6. Surface area expansion of Lake Baringo between 1984 and 2018. ENSO events that occurred during that period are marked by faded gray bars.

0.96. The primary output of the study is comparison maps of land cover culminating in change detection maps (Figs. 4 and 5). All the different datasets point to a significant change in land cover involving the water class that dramatically takes place after 2010. The classification results show that surface areas of all the four Rift valley lakes were substantially more extensive in 2016 when compared to the period before 2010. After experimenting with different indices, the MNDWI proved to be the most robust in delineating water surfaces. Subsequently, the MNDWI was adopted for presenting surface areas of the lakes because its results were found to be comparable to those attained through both supervised and unsupervised classifications. Whereas the NDVI was successful for delineating water surface at Lake Baringo, it proved ill-equipped for that purpose in Lakes Bogoria, Nakuru, and Elementaita whose surfaces were dominated by significant coverage for algae for much of the period that was studied. However, the NDVI proved valuable when estimating the surface area of the lakes that were covered by algae.

As shown in Table 3, the surface area of Lake Baringo that was computed through MNDWI was 149 km² in 1984 before it decreased to 120 km² in 1995 and 112 km² in 2003. The surface area of the lake did not increase above the 1984 level, even during major ENSO events,

until after 2010 (Fig. 6). Lake Baringo's surface area increased from 136 km² in 2010 to 193 km² in 2014. A similar trend is evident when NDVI is utilized to calculate the surface area for Lake Baringo albeit with some underestimation (Table 3). MNDWI shows that Lake Nakuru whose surface area was 42.7 km² in 1984, decreased to 33.7 km² in 1995 and remained low until after 2010 when it increased from 34.6 km² to 54.2 km² in 2014. The NDVI values mostly exhibit a negative correlation with the lake surface area at Lake Nakuru. Much of its surface was characterized by positive NDVI values (= or >0.1), which was confirmed to be consistent with vegetation (algae) cover during the period between 1986 and 2010 (Fig. 7, Table 4). However, the algae disappeared in 2014 concurrent with increased lake surface area. Algae covered 43 km² of Lake Nakuru in 1984 before decreasing to a low of 22 km² in 1989. Overall, algae cover averaged 30 km² until 2010. The surface area of the lake that was covered by algae was <1 km² between 2014 and 2018 which corresponds with an algal collapse of 95% when compared to the 2010 values.

Lake Bogoria's surface displays a dichotomous pattern of consistency in its surface area. Between 1984 and 2010 the surface area varied between 30 km² and 33 km² (Fig. 8). Its surface area increased to 39 km² in 2014 and remained mostly above 38 km² for the following

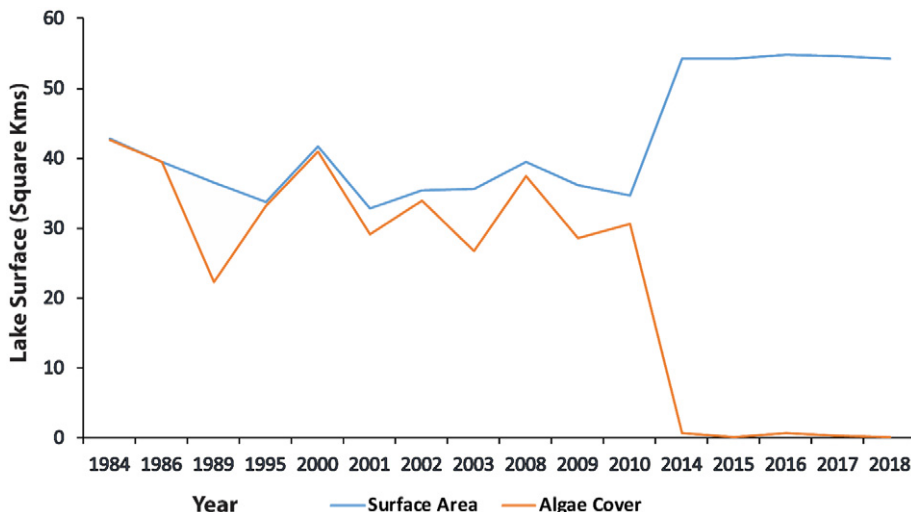


Fig. 7. The surface area of Lake Nakuru between 1984 and 2018 marked by the blue line. The surface area of the lake covered by algae during that period is marked by the orange line.

Table 4

Lake surface area (km^2) covered with Algae computed using NDVI (values = or >0.1).

Year	Bogoria	Elementaita	Nakuru
1984	30.1	4.8	42.64
1986	15.2	2.9	39.4
1989	13.1	17.7	22.4
1995	25.7	9.7	33.2
2000	21	19	41
2001	32.7	12.6	29.1
2002	33.4	17.8	33.9
2003	26.2	6.6	26.8
2008	32	7.2	37.4
2009	32.1	4.7	28.5
2010	27.1	13.3	30.7
2014	5.3	0.9	0.7
2015	1.9	1.9	0.2
2016	1.2	6.7	0.7
2017	7	0.5	0.3
2018	2	0.8	0.2

four years. Algae covered 30 km^2 or 91% of Lake Bogoria in 1984. Although the lowest surface area covered by algae was 13 km^2 in 1989, the cover averaged above 25 km^2 for the period before 2010. In 2014 algae cover in Lake Bogoria dramatically declined to 5 km^2 and continued to disappear in subsequent years.

Lake Elementaita's surface area is characterized by fluctuations throughout the thirty-four years covered in this study albeit with consistency in the last four years (Fig. 9). The water surface area was 18.6 km^2 in 1984, dropping slightly to 17.7 km^2 before recovering to 19.3 km^2 in 1986 and 1988, respectively. The lake's surface area decreased to 16.6 km^2 in 1995 and then rose to 20.5 km^2 in 2000 before dropping to 15.5 km^2 in 2001. Over the next decade, Lake Elementaita's surface area never increased beyond 19 km^2 . Its surface area was 16 km^2 in 2010 before it expanded to 22 km^2 in 2014, which corresponds with a 38% increase over the four years and has remained above 21 km^2 since. Algae cover on Lake Elementaita showed more fluctuations than in the other lakes albeit with the same negative correlation with lake surface area. Algae covered 5 km^2 or 26% of Lake Elementaita in 1984 before decreasing to 3 km^2 in 1986 and then rebounding to 18 km^2 in 1989. Between 1995 and 2010 the average cover was 11 km^2 with a low of 5 km^2 (in 2009) and a high of 19 km^2 (in 2000). However, in 2014 the lake surface area that was covered by algae dramatically decreased to 1 km^2 and continued to be suppressed in subsequent years, averaging <2 km^2 or 0.1% of the lake (Fig. 9).

Although all the four lakes displayed significant changes in the surface area over three decades, the results show that the most substantial changes occurred in Lakes Nakuru and Baringo after 2010. For that reason, the drainage basins of these two lakes were scrutinized in detail for changes in land cover that could help explain the dramatic changes in the surface area that occurred after 2010. Tables 5 and 6 summarize changes in land cover in the watersheds between 2010 and 2016 at Lakes Nakuru and Baringo, respectively. About 2% of the Lake Nakuru watershed is urban whereas the Lake Baringo has no significant urban cover class. The drainage basins of these lakes are dominated by grassland and farms class which constitutes over 60% and 40% for Nakuru and Baringo, respectively. Forests occupy about 20% of the two watersheds. To further help explain the changes at the lakes we reviewed the rainfall data from stations located in the vicinity of these lakes (Figs. 10, and 11).

4. Discussion

4.1. Change in lake surface area

Land cover change remains an essential marker for assessing human and natural impacts on ecosystems, surface processes, and environmental change at regional and global scales (Hersperger et al., 2018; Magliocca et al., 2015). The results from this study provide evidence for land cover change, especially surface area changes in the Rift valley lakes. The temporal pattern of change in lake size falls into two categories, i.e., a phase of gradual but steady decline in surface area between 1984 and 2010 and a phase of dramatic increase in size from 2010 to present. As already noted, the MNDWI proved to be the most reliable method of delineating water surfaces by consistently proving results that matched those attained from supervised and unsupervised classifications. Lake Baringo declined from 149 km^2 in 1984 to 112 km^2 in 2003 (Table 3) which corresponds with a reduction of 25% of the lake surface area in about 20 years. After the 2003 low, the surface area at Lake Baringo somewhat increased, rising to 136 km^2 in 2010 but never returned to its 1984 size. During the period of dramatic decline in surface area epitomized by the 2003 size, it was reported that Lake Baringo would dry up within 15 years due to a combination of land degradation and high sedimentation rates (Kurgat, 2003). Kiage et al. (2007) could not confirm those projections. Nonetheless, Kiage et al. (2007) observed significant changes in land cover due to deforestation concurrent with land degradation, increased soil erosion and sediment yield in the Lake Baringo drainage basin. Between 2010 and 2014 Lake Baringo's

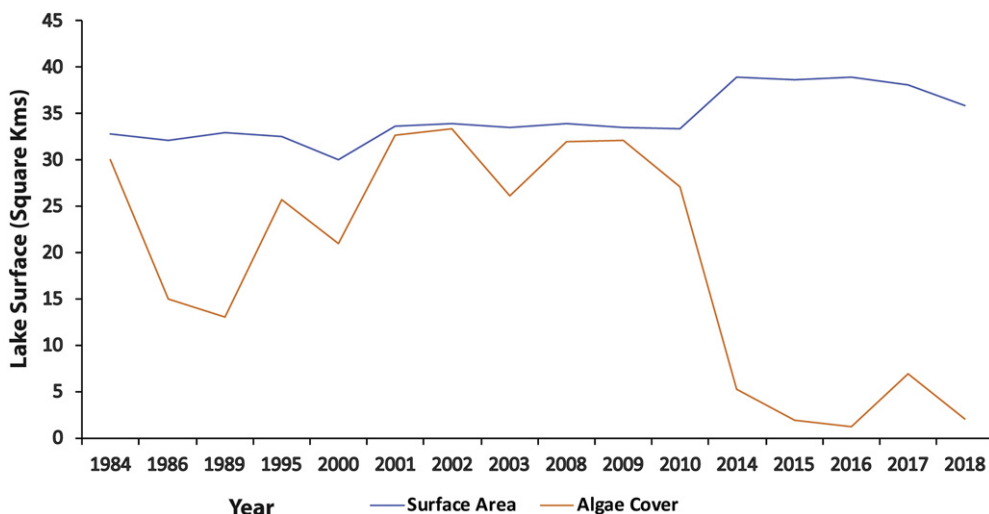


Fig. 8. The surface area of Lake Bogoria between 1984 and 2018 marked by the blue line. The surface area of the lake covered by algae during that period is marked by the orange line.

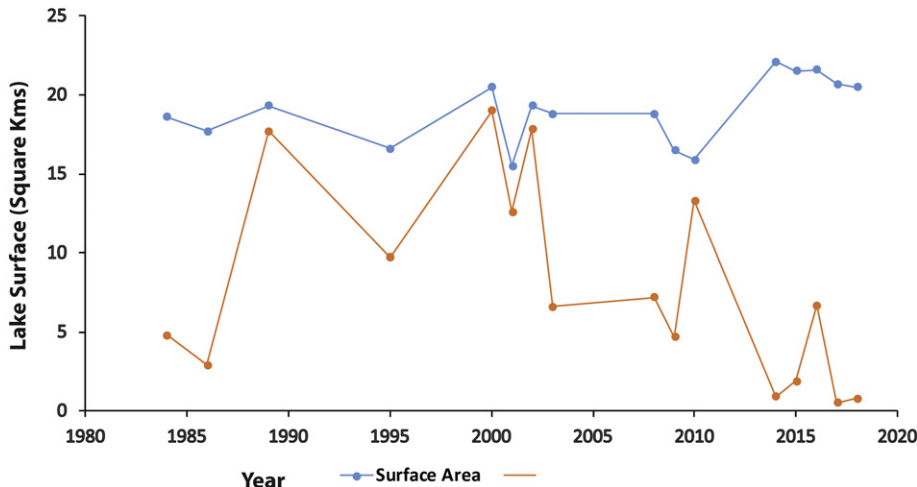


Fig. 9. The surface area of Lake Elementaita between 1984 and 2018 marked by the blue line. The surface area of the lake covered by algae during that period is marked by the orange line.

surface area increased to 193 km², which is consistent with a change of 42% in 4 years.

The same pattern of change is replicated at Lakes Bogoria and Elementaita, but even more so at Lake Nakuru. The latter experienced an increase of 57% between 2010 and 2014, rising from 35 km² to 54 km². The change in the surface area at Lakes Bogoria and Elementaita between 2010 and 2014 was an increase of 18% and 38%, respectively. The suppressed increase in Lake Bogoria's surface area, when compared to the other lakes, is mostly due to the fact that the lake occupies a deep and, somewhat, narrow depression which experienced a rise in lake level but was accompanied by limited expansion in surface area when compared to the shallow depressions occupied by the other lakes. The increase in surface area at Bogoria is restricted to the shorelines in the northern part of the lake. Obando et al. (2016) estimated the surface area at Lake Baringo to have increased by 53%, which is almost 10% higher than the figures seen in this study. At Lakes Bogoria and Nakuru, their estimate was an increase of 24% and 76%, respectively, between

2010 and 2014. Obando et al. (2016) did not subject their imagery to atmospheric correction. It is, therefore, possible their higher estimates of lake sizes are a product of classification error which can arise whenever the atmospheric correction is not performed.

Although data on bathymetry changes at the four lakes are not available, there is no doubt that the increase in the surface areas of these lakes must be accompanied a rise in lake level. It is possible to make estimates of change in lake level by using features or landmarks that were previously near the shorelines but which are now submerged in these lakes. At Lake Nakuru, for instance, the National Parks head office buildings which were previously located about 1 km from the lake's shoreline were in the process of being submerged in 2014 (Figs. 12 and 13). Therefore, using satellite remote sensing and field observation, the depth is estimated to have risen at least 1.5 to 2 m above the 2010 lake level. It is, therefore, no surprise that the remarkable increase in surface area has led to the loss of property and livelihoods as the lake waters took over adjacent villages, schools, and other property.

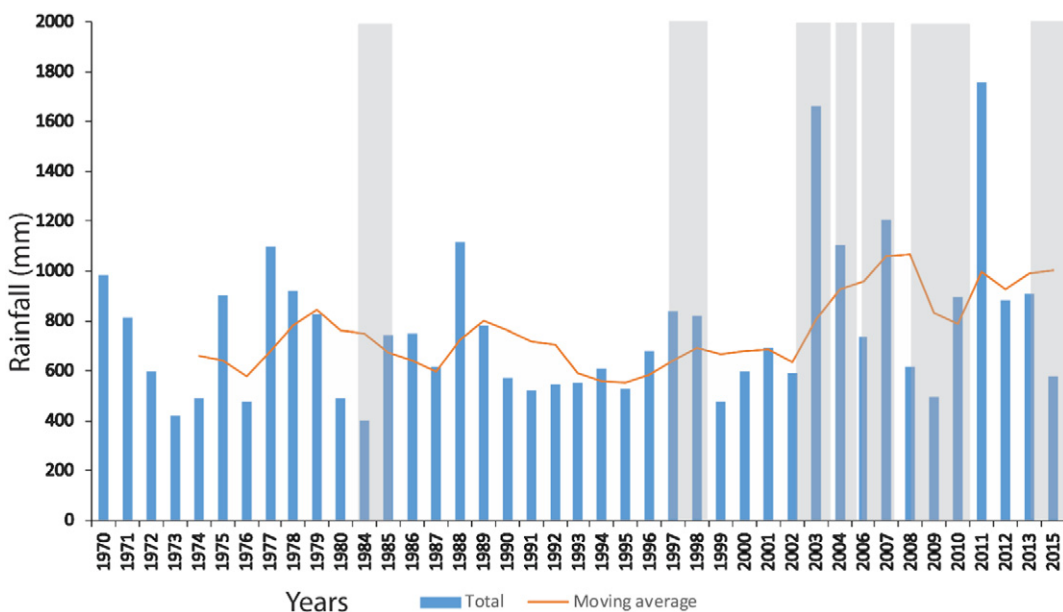


Fig. 10. Rainfall data derived from Snake Farm Meteorological station on the shores of Lake Baringo (970 m above sea level). The blue bars present the total annual rainfall while the line graph tracks the moving average. ENSO years are highlighted by gray bars.

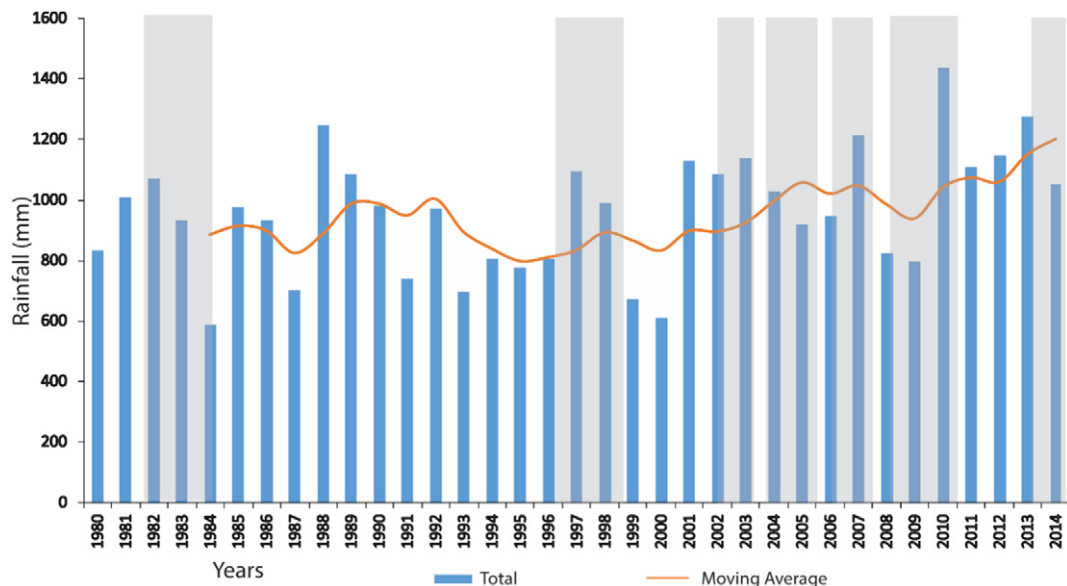


Fig. 11. Rainfall data derived from Nakuru station (at 1915 m above sea level). The blue bars present the total annual rainfall while the line graph tracks the moving average. ENSO years are highlighted by gray bars.

4.2. Land cover and land use change

Many factors can explain the expansion of the Rift Valley lakes after 2010. These factors include climate change, land cover changes due to human activities in the drainage basins, and tectonic activity. Different satellite image enhancements highlighted differences in the various land cover classes. The study shows that all the land cover classes in the region changed. Land cover classes that are common in both watersheds are grassland/farms, forest, scrubland/woodland, water, and bare ground. The Lake Baringo watershed is devoid of any significant urbanized area and, therefore, the urban/cultural land cover is only limited to the Lake Nakuru watershed.

Change detection analyses of land cover classification maps for 2010 and 2014 provide useful data for assessing change in land cover during that period. As expected the water class was the land cover class that experienced the most turnover in the Lake Nakuru watershed increasing from 32 km² in 2010 to 55 km² in 2014. Urban land cover increased from 46 km² to 67 km², which translates to an increase of 46% concurrent with an expansion of scrubland/woodland cover. The latter experienced a rise of 34% by expanding from 80 km² in 2010 to 108 km² in 2014. Both grassland/farms and forest land cover classes experienced a 5% decrease between 2010 and 2014. The meager 5% decrease in the grassland/farms and forest land cover masks the enormity of change considering the two are the largest land cover classes in the watershed. For perspective, the percentage change in the grassland/farmland cover translates to about 56 km², which is slightly more than the surface area covered by water (that is, the total area occupied by water in the lake, rivers, artificial reservoirs, and sewerage treatment plants in the entire watershed). Most of the change in the grassland/farm was conversion to the bare land class mainly because the open grasslands transitioned from pastureland to cultivated crop farms. Expansion of the urban land cover accounts for much of the remainder of the change in the grassland/farms. The difference in the forest class is primarily due to deforestation as land that was occupied by forests in 2010 got converted to farmland or settlement or transitioned to the scrubland/woodland cover in 2014 as large trees were harvested.

A similar pattern of change in land cover is evident in the Lake Baringo watershed, albeit with unique differences and without the urban land cover. The results of the land cover classification confirm the expansion of the water class between 2010 and 2014. It is important

to note that surface area changes to land cover in the Lake Baringo watershed are much more significant when compared to the Lake Nakuru watershed. The most significant change occurred in forest land cover which decreased from 175 km² in 2010 to 125 km² in 2014, which is consistent with a reduction of 29% over the four years. Although some of the changes in the forest cover are due to conversion into farmland which, partially also partially explains the increase in bare ground land cover, that would only account for only a small proportion of the change. This study shows that most of the forest land cover transitioned to scrub/woodland as harvesting of mature trees led more open forests that ended up recording a spectral signature that is similar to that of the scrub/woodland land cover. Grasslands/farms land cover which is the largest land cover class (accounting for about 50% of the watershed) experienced a change of 7%, decreasing from 2838 km² in 2010 to 2633 km² in 2014. Conversion to bare ground and transition to scrubland accounts for the bulk of the change in the grassland/farms land cover during the period of study.

Watersheds can be extremely sensitive to land cover and land use dynamics with significant impacts on river flow and sediment yields (Welde and Gebremariam, 2017; Zhu and Li, 2014). Change detection analyses of land cover classification maps for 2010, and 2014 shows significant changes in land cover and land use in the drainage basins of Lakes Baringo and Nakuru that probably contributed to the expansion their lake surface areas. Change in land cover has the potential to alter the balance between rates of infiltration and run-off, which can transform surface hydrological processes (Shi et al., 2007). The rapid expansion of urban areas is often characterized by a decrease in surface roughness and a comparable increase in impermeable surfaces such as

Table 5

Coverage of different land cover types based on unsupervised classification and change detection for Lake Nakuru drainage basin.

Land cover type	Coverage in hectares			
	2010	2016	Change	% Change
Water	3145	5519	2311	57
Bare ground	14,866	15,071	205	1
Grassland/farms	111,338	105,786	-5552	-5
Scrubland/woodland	7961	10,700	2739	34
Urban	4576	6693	2117	46
Forest	33,333	31,513	-1820	-5

Table 6

Coverage of different land cover types based on unsupervised classification and change detection for Lake Baringo drainage basin. The basin does incorporate any major urban area.

Land cover type	Coverage in sq. kilometers			
	2010	2016	Change	% Change
Water	13,892	19,944	6052	44
Bare ground	10,200	14,401	4201	41
Grassland/farms	283,756	263,371	-20,385	-7
Scrubland/woodland	126,238	186,144	59,906	47
Forest	174,637	124,863	-49,774	-29

roads and buildings all of which can drastically reduce the capacity of rainfall detention and sharply increase runoff and erosion. Considering that Lake Nakuru watershed experienced a 46% increase in urban land cover between 2010 and 2014, it is possible that some of the changes in the lake surface area are a direct contribution from increased runoff from the city of Nakuru. Multiple studies have demonstrated that modification of land for construction can increase soil erosion to over 4000 times higher than the preconstruction rates (Zhu and Li, 2014;

McClintock and Harbor, 1995; Harbor, 1999). This may suggest that urbanization and other human activities will not only be accompanied by increased runoff but the sediment yield that comes with the runoff can have a significant effect on shallow basins such as those that define the Rift valley lakes.

Although the Baringo watershed is predominantly rural, it has small towns that would also contribute to the increased runoff, but their contribution would be insignificant. Urban input to surface runoff in the two watersheds is unlikely to match the input from surface areas that were previously covered by forests or grasslands both of which account for over two-thirds of land cover.

The adverse changes in the forest land cover can be attributed to deforestation mainly to expand farmland, which is a critical resource for the livelihoods of the local population. Loss of forest and grassland cover has a significant impact on surface hydrology because vegetation acts both as a "pump" (enhance evapotranspiration) and a "sponge" (increase infiltration) (Guzha et al., 2018). Loss of forest land cover and change in land use in the study area can account for part of the expansion in the Rift valley lakes because forest loss has been shown to increase surface runoff, elevate soil erosion rates, and elevate both mean



Fig. 12. Digital Globe satellite images from Google Earth covering the northeastern shoreline of Lake Nakuru. Panel A which was acquired in January 2010 shows a building of Lake Nakuru National Park head offices indicated by a red circle with a red arrow pointing to it. The shoreline was about 800 m away from the buildings. Panel B is the same area in January 2014 with the National Park office building taken up by the lake.



Fig. 13. A picture of the National Park building shown in Fig. 12 in the process of being submerged, taken by the author during a visit in December 2013. All the trees were part of the forest that previously fringed the lake have since died due to saltwater inundation.

annual and peak river discharges (Guzha et al., 2018). However, it is unlikely that spatial and temporal change in land cover alone would account for the substantial expansion of surface area that has been experienced in the Rift valley lakes since 2010. Transformation of land cover due to development of urbanization, deforestation, and agriculture has been on-going in the region, including the period since 1984

that was examined in this study using satellite imagery yet no marked changes in lake surface area occurred until after 2010. Dynamics in lake levels and surface areas are controlled by the water balance, which is a function of precipitation on the lake, evaporation, inflow and outflow from rivers. There is a need, therefore, to investigate other forcing mechanisms to explain the change in lake levels.



Fig. 14. Some of the few flamingos that are still left on the shores of Lake Nakuru [Picture was taken by the author in December 2013].

According to the International Panel on Climate Change (IPCC) Fourth Assessment Report, changes in lake levels can be ascribed to human activities and precipitation changes (IPCC, 2007).

4.3. Collapse of algae cover

Precipitation data from meteorological stations located near the four lakes since 1980 shows continuous variability with peaks that can be linked with occurrence ENSO events (Figs. 10 and 11). Effects of the ENSO episodes of 1997–1998, 2002–03, 2004–05, 2006–07, 2009–10 are evident in the precipitation character. The moving average of the data shows an uptick in rainfall beginning 2006–2015. Lake surface area largely tracks the precipitation pattern. For instance, the periods of suppressed precipitation between 1995 and 2003 correspond with the marked decrease in lake surface area while the periods of high rainfall after 2003 were accompanied by an increase in lake surface area (2008–2010). This study shows that the major ENSO events of 1982–1983 and 1997–1998, which were accompanied by enhanced rainfall that caused floods in many parts of Kenya only led to minimal changes in lake levels. Total rainfall from the most recent major ENSO event (2014–2016) was not significantly different from the records from previous ENSO events. Therefore, rain from the 2014–2016 ENSO event alone cannot fully account for the changes reflected in the lake surface areas. It is possible that cumulative increase in rainfall that began after 2003 may partially explain the difference in lake levels, especially when coupled with remarkable changes in land use and land cover. However, rainfall data from the region does not reveal any abrupt changes in precipitation pattern after 2010 that would trigger the kind of change in surface area in the four Rift Valley lakes.

Considering that rainfall coupled with changes in land use and land cover do not fully account for the differences in lake levels then the contribution from groundwater sources could be an alternative contributing factor. In many cases, lakes lose water through underground seepage (Odongo et al., 2015). For instance, the waters of Lake Baringo remain fresh despite lack of a visible outlet because of significant underground seepage through fractured lake floor (Omondi et al., 2016). However, a considerable part of the water budget at Lakes Bogoria, Elementaita, and Nakuru is inflow from springs. These lakes are primarily of tectonic origin, having developed along linear faults across an ancient geologic landscape that has been reworked by recent volcanic activity (Fazi et al., 2018). It is possible that a tectonic event could trigger a change in geogenic water input that would, in the context of increased rainfall and changes in land cover and land use, affect lake levels. This warrants investigations on tectonic activity within the Rift Valley and its impacts on groundwater flow to solidify it as part of the matrices that can explain the surface area changes.

The increase in water levels appears to have altered the chemical balance of the hypersaline lakes that could have severe ramifications on the biodiversity of the lakes, which are thought to be a cradle avian biodiversity (Fazi et al., 2018). Life in the Rift Valley lakes is a delicate equilibrium which, if altered can decimate their fragile ecosystems. An important marker for the changing lake biogeochemistry is the pattern of algae cover, especially in the hypersaline lake environments of Bogoria, Elementaita, and Nakuru. This study shows an inverse correlation between change in lake surface area and algae coverage, characterized by steady algae cover in the period leading up to 2010 followed by a sharp decline thereafter. Algae (*Arthrospira fusiformis* and *A. fusiformis-P. minor*), a colony of blue-green bacteria (cyanobacteria) whose assembly is visible as tiny flakes by the naked eye, is the primary diet of the large flocks of pink flamingos that for a long time were ubiquitous in Lakes Nakuru, Elementaita and Bogoria. The population of the flamingos has since plummeted (Fig. 14) following periods of suspected heavy metal pollution and, now, the possible changes in the water chemistry after 2010.

Forecasting and explaining the components that control the hydrology of the Rift Valley lakes constitute a growing challenge. Greater

research effort is required to perform detailed analysis of water chemistry to ascertain the exact magnitude of change in the biogeochemical composition of the lakes due to changes that began in 2010. The findings of this study provide observations that offer some valuable insights into potential causes for the spatiotemporal changes in land cover in the drainage basins and their contribution to changes in lake surface area. However, it is imperative that interdisciplinary investigations be performed to provide information to test for any trends in the nature and character of geogenic contribution and impacts on ecosystem services rendered by changes in the Rift Valley lakes. There is urgent need for interdisciplinary research to provide cogent solutions and measures to mitigate looming environmental catastrophe in the Rift Valley lake ecosystems.

5. Conclusions

This study has documented the expansion of Rift valley lakes over the past thirty-four years using satellite images acquired by Landsat TM, ETM+, and OLI. The MNDWI was adopted for delineating water surface areas after proving to be more accurate and robust when compared to the output of NDVI and classification algorithms. The findings from satellite remote sensing confirm the changes in the surface area in the Rift Valley lakes after 2010. The remarkable rise in lake levels and expansion of surface area after 2010 that have submerged surrounding areas disrupting livelihoods, damaging property, and displacing thousands of people appear to have multiple causations including land cover and land use change, cumulative increase in rainfall, and a possible change in geogenic water input due to some tectonic activity.

This study shows that all land cover types experienced marked change that could partially explain the dynamics in the surface area of the Rift Valley lakes. There was a decrease in vegetation cover (forests and grasslands) due to the expansion of agricultural lands. This study also shows an increase in bare grounds and urban land cover. Removal of vegetation cover due to development of agriculture and urbanization in the lake watersheds were likely to have precipitated both increases in runoff and sediment yield with a profound effect on shallow basins that define the Rift valley lakes. This study suggests the possibility that some tectonic activity may have opened the floodgates of the groundwater recharge systems which in combination with land cover and use change and the cumulative effect of enhanced rainfall after 2006 contributed to the remarkable expansion of the lake surface areas. However, more studies are warranted to assess the potential role of tectonic activity in influencing groundwater recharge before it is moved from speculation to become part of the matrix of factors that explain changes in lake surface area that began after 2010. What is alarming is the potential threat to the rich biodiversity and impacts on ecosystem services of the Rift Valley lakes.

Declaration of competing interest

The authors (Lawrence Kiage and Paul Douglas) declare that he has no known competing financial interests or personal relationships that could have appeared to influence the work reported in this paper.

Acknowledgements

The primary data that were analyzed for this project are satellite imagery that were acquired from the United States Geological Survey (USGS). The data are freely available and can be downloaded from the EarthExplorer portal by clicking on <https://earthexplorer.usgs.gov/>. We extend our gratitude to the anonymous reviewers and the editors for their discussion and comments that significantly improved the quality of this paper. Permission to conduct this research was granted by the Uganda National Council for Science and Technology and local government leaders. We thank Mrs. Carole Kiage of the Kenya Wildlife Service,

who facilitated the fieldwork in Lake Nakuru National Park. We also thank Mrs. Christine Mahonga of the Kenya Meteorological Service and her staff for her assistance with the rainfall data.

References

- Acharya, T.D., Subedi, A., Lee, D.H., 2018. Evaluation of water indices for surface water extraction in a Landsat 8 scene of Nepal. *Sensors* 18. <https://doi.org/10.3390/s18082580>.
- Alamgir, A., Khan, M.A., Manino, I., Shaukat, S.S., Shahab, S., 2016. Vulnerability to climate change of surface water resources of coastal areas of Sindh, Pakistan. *Desalin. Water Treat.* 57, 18668–18678.
- Berk, A., Bernstein, L.S., Anderson, G.P., Acharya, P.K., Robertson, D.C., Chetwynd, J.H., Adler-Golden, S.M., 1998. MODTRAN cloud and multiple scattering upgrades with application to AVIRIS. *Remote Sens. Environ.* 65, 367–375.
- Buma, W.G., Lee, S.I., Seo, J.Y., 2018. Recent surface water extent of Lake Chad from multispectral sensors and GRACE. *Sensors* 18, 24. <https://doi.org/10.3390/s18072082>.
- Congalton, R.G., Green, K., 1999. Assessing the Accuracy of Remotely Sensed Data: Principles and Practices. Lewis, Boca Raton, FL.
- Dünnforth, M., Bergner, A.G.N., Trauth, M.H.J., 2006. Early Holocene water budget of the Nakuru-Elmenteita basin, Central Kenya. *Rift. J. Paleolimnol.* 36 (3), 281–294.
- Fazi, S., Butturini, A., Tassi, F., Amalfitano, S., Venturi, S., Vazquez, E., Clokie, M., Wanjal, S.W., Pacini, N., Harper, D.M., 2018. Biogeochemistry and biodiversity in a network of saline-alkaline lakes: implications of ecohydrological connectivity in the Kenyan Rift Valley. *Ecohydrology & Hydrobiology* 18, 96–106.
- Gao, H., Birkett, C., Lettenmaier, D.P., 2010. Global monitoring of large reservoir storage from satellite remote sensing. *Water Resour. Res.* 48, 12. <https://doi.org/10.1029/2012WR012063>.
- Guzha, A.C., Rufino, M.C., Okoth, S., Jacobs, S., Nobrega, R.L.B., 2018. Impacts of land use and land cover change on surface runoff, discharge and low flows: evidence from East Africa. *Journal of Hydrology-Regional Studies* 15, 49–67.
- Halabisky, M., Moskal, L.M., Gillespie, A., Hannam, M., 2016. Reconstructing semi-arid wetland surface water dynamics through spectral mixture analysis of a time series of Landsat satellite images (1984–2011). *Remote Sens. Environ.* 177, 171–183.
- Harbor, J., 1999. Engineering geomorphology at the cutting edge of land disturbance: erosion and sediment control on construction sites. *Geomorphology* 31, 247–263.
- Hersperger, A.M., Oliveira, E., Pagliarin, S., Palka, G., Verburg, P., Bolliger, J., Grdinariu, S., 2018. Urban land-use change: the role of strategic spatial planning. *Global Environmental Change-Human and Policy Dimensions* 51, 32–42.
- Inter-Governmental Panel on Climate Change (IPCC), 2007. Climate change 2007. Synthesis Report (IPCC, Geneva). Contribution of Working Groups I, II and III to the Fourth Assessment Report of the Intergovernmental Panel on Climate Change. 7. IPCC, Geneva, Switzerland.
- Jiang, S.Y., Xiong, Q.X., Zhu, J.Q., 2014. Evaluation of lake eutrophication based on the HJ-1 satellite multispectral data. In: Yarlagadda, P., Choi, S.B., Kim, Y.H. (Eds.), Computer and Information Technology. Trans Tech Publications Ltd, Stafa-Zurich, pp. 1184–1187.
- Jiang, Z.L., Qi, J.G., Su, S.L., Zhang, Z.H., Wu, J.P., 2012. Water body delineation using index composition and HIS transformation. *Int. J. Remote Sens.* 33, 3402–3421.
- Kiage, L.M., Obuyoyo, J., 2011. The potential link between El Niño and water hyacinth blooms in Winam gulf of Lake Victoria, East Africa: evidence from satellite imagery. *Water Resour. Manag.* 25, 3931–3945.
- Kiage, L.M., Walker, N.D., 2009. Using NDVI from MODIS to monitor duckweed bloom in Lake Maracaibo, Venezuela. *Water Resour. Manag.* 23, 1125–1135.
- Kiage, L.M., Liu, K., Walker, N.D., Lam, N., Huh, O.K., 2007. Recent land-cover/use change associated with land degradation in the Lake Baringo catchment, Kenya, East Africa: evidence from Landsat TM and ETM+. *Int. J. Remote Sens.* 28, 4285–4309.
- Krienitz, L., Mahnert, B., Schagerl, M., 2016. Lesser flamingo as a central element of the east African avifauna. In: Schagerl, M. (Ed.), Soda Lakes of East Africa. Springer, Cham. https://doi.org/10.1007/978-3-319-28622-8_10.
- Kurgat, M., (2003). Lake Baringo drying up-UNDP. The East African Standard. 10 April 2003. Available online at: <http://216.185.134.103/archives/april/thur10042003/headlines/news10042003015.htm> (accessed 2 November 2006).
- LaVigne, M., Ashley, G.M., 2002. Climatology and Rainfall Patterns: Lake Bogoria National Reserve (1976–2001). Department of Geological Sciences, Rutgers University, Piscataway, NJ, U.S.A.
- Liang, K., Yan, G.Z., 2017. Application of Landsat imagery to investigate lake area variations and relict Gull Habitat in Hongjian Lake, Ordos Plateau, China. *Remote Sens.* 9. <https://doi.org/10.3390/rs9101019>.
- Magliocca, N.R., Rudel, T.K., Verburg, P.H., McConnell, W.J., Mertz, O., Gerstner, K., Heinemann, A., Ellis, E., 2015. Synthesis in land change science: methodological patterns, challenges, and guidelines. *Reg. Environ. Chang.* 15, 211–226.
- McClintock, K., Harbor, J.M., 1995. Modeling potential impacts of land development on sediment yields. *Phys. Geogr.* 16, 359–370.
- Mohammadi, A., Costelloe, J.F., Ryu, D., 2017. Application of time series of remotely sensed normalized difference water, vegetation and moisture indices in characterizing flood dynamics of large-scale arid zone floodplains. *Remote Sens. Environ.* 190, 70–82.
- Murimi, S.K., 1993. The drying up of the East African Rift Valley lakes in recent times: the case of Lake Elementaita. *Journal of Eastern African Research & Development* 23, 40–62.
- Obando, J.A., Onywere, S., Shisanya, C., Ndubi, A., Masiga, D., Irura, Z., Mariita, N., Maragua, H., 2016. In: Meadows, M.E., Lin, J.C. (Eds.), Impact of Short-Term Flooding on Livelihoods in the Kenya Rift Valley Lakes. Geomorphology and Society, pp. 193–215.
- Odongo, V.O., van der Tol, C., van Oel, P.R., Meins, F.M., Becht, R., Onyango, J., Su, Z.B., 2015. Characterisation of hydroclimatological trends and variability in the Lake Naivasha basin, Kenya. *Hydrol. Process.* 29, 3276–3293.
- Omondi, R., Ojwang, W., Olilo, C., Mugambi, S., Ojuok, J.E., 2016. Lakes Baringo and Naivasha: Endorheic freshwater lakes of the Rift Valley (Kenya). In: Finlayson, C., Milton, G., Prentice, R., Davidson, N. (Eds.), The Wetland Book. Springer, Dordrecht.
- Raini, J.A., 2009. Impact of land use changes on water resources and biodiversity of Lake Nakuru catchment basin, Kenya. *Afr. J. Ecol.* 47, 39–45.
- Renaut, R.W., Owen, R.B., Ego, J.K., 2017. Geothermal activity and hydrothermal mineral deposits at southern Lake Bogoria, Kenya Rift Valley: impact of lake level changes. *J. Afr. Earth Sci.* 129, 623–646.
- Rokni, K., Ahmad, A., Selamat, A., Hazini, S., 2014. Water feature extraction and change detection using multitemporal Landsat imagery. *Remote Sens.* 6, 4173–4189.
- Scharsich, V., Mtata, K., Haups, M., Lange, H., Bogner, C., 2017. Analysing land cover and land use change in the Matobo National Park and surroundings in Zimbabwe. *Remote Sens. Environ.* 194, 278–286.
- Shi, P.J., Yuan, Y., Zheng, J., Wang, J.A., Ge, Y., Qiu, G.Y., 2007. The effect of land use/cover change on surface runoff in Shenzhen region, China. *Catena* 69, 31–35.
- Toure, S.I., Stow, D.A., Shih, H.C., Weeks, J., Lopez-Carr, D., 2018. Land cover and land use change analysis using multi-spatial resolution data and object-based image analysis. *Remote Sens. Environ.* 210, 259–268.
- Wang, X.B., Xie, S.P., Zhang, X.L., Chen, C., Guo, H., Du, J.K., Duan, Z., 2018. A robust Multi-Band Water Index (MBWI) for automated extraction of surface water from Landsat 8 OLI imagery. *Int. J. Appl. Earth Obs. Geoinf.* 68, 73–91.
- Wang, Y.C., Feng, C.C., 2011. Patterns and trends in land-use land-cover change research explored using self-organizing map. *Int. J. Remote Sens.* 32, 3765–3790.
- Welde, K., Gebremariam, B., 2017. Effect of land use land cover dynamics on hydrological response of watershed: case study of Tekeze Dam watershed, northern Ethiopia. *International Soil and Water Conservation Research* 5, 1–16.
- Xu, H.Q., 2006. Modification of normalised difference water index (NDWI) to enhance open water features in remotely sensed imagery. *Int. J. Remote Sens.* 27 (14), 3025–3033.
- Yang, X.C., Qin, Q.M., Grussenmeyer, P., Koehl, M., 2018. Urban surface water body detection with suppressed built-up noise based on water indices from Sentinel-2 MSI imagery. *Remote Sens. Environ.* 219, 259–270.
- Zhang, H.K., Roy, D.P., 2016. Landsat 5 Thematic Mapper reflectance and NDVI 27-year time series inconsistencies due to satellite orbit change. *Remote Sens. Environ.* 186, 217–233.
- Zhang, J.X., Zhang, W.L., Mei, Y.Y., Yang, W.J., 2019. Geostatistical characterization of local accuracies in remotely sensed land cover change categorization with complexly configured reference samples. *Remote Sens. Environ.* 223, 63–81.
- Zhu, C., Li, Y., 2014. Long-term hydrological impacts of land use/land cover change from 1984 to 2010 in the Little River Watershed, Tennessee. *International Soil and Water Conservation Research* 2, 11–22.